COMPUTING THE GROUND STATE SOLUTION OF BOSE–EINSTEIN CONDENSATES BY A NORMALIZED GRADIENT FLOW*

WEIZHU BAO† AND QIANG DU‡

Abstract. In this paper, we present a continuous normalized gradient flow (CNGF) and prove its energy diminishing property, which provides a mathematical justification of the imaginary time method used in the physics literature to compute the ground state solution of Bose–Einstein condensates (BEC). We also investigate the energy diminishing property for the discretization of the CNGF. Two numerical methods are proposed for such discretizations: one is the backward Euler centered finite difference (BEFD) method, the other is an explicit time-splitting sine-spectral (TSSP) method. Energy diminishing for BEFD and TSSP for the linear case and monotonicity for BEFD for both linear and nonlinear cases are proven. Comparison between the two methods and existing methods, e.g., Crank–Nicolson finite difference (CNFD) or forward Euler finite difference (FEFD), shows that BEFD and TSSP are much better in terms of preserving the energy diminishing property of the CNGF. Numerical results in one, two, and three dimensions with magnetic trap confinement potential, as well as a potential of a stirrer corresponding to a far-blue detuned Gaussian laser beam, are reported to demonstrate the effectiveness of BEFD and TSSP methods. Furthermore we observe that the CNGF and its BEFD discretization can also be applied directly to compute the first excited state solution in BEC when the initial data is chosen as an odd function.

Key words. Bose–Einstein condensate, nonlinear Schrödinger equation, Gross–Pitaevskii equation, ground state, continuous normalized gradient flow, monotone scheme, energy diminishing, time-splitting spectral method

AMS subject classifications. 35Q55, 65T40, 65N12, 65N35, 81-08

DOI. 10.1137/S1064827503422956

1. Introduction. Since the first experimental realization of Bose–Einstein condensates (BECs) in dilute weakly interacting gases, the nonlinear Schrödinger (NLS) equation, also called the Gross–Pitaevskii equation (GPE) [26, 31], has been used extensively to describe the single particle properties of BECs. The results obtained by solving the NLS equation showed excellent agreement with most of the experiments (for a review see [3, 14, 15]). In fact, up to now there have been very few experiments in ultracold dilute bosonic gases which could not be described properly by using theoretical methods based on the NLS equation [22, 25].

There has been a series of recent studies which deal with the numerical solution of the time-independent GPE for ground state and the time-dependent GPE for finding the dynamics of a BEC. For numerical solutions of time-dependent GPE, Bao et al. [4, 5, 7, 8] presented a time-splitting spectral method, Ruprecht et al. [33] used the Crank–Nicolson finite difference method to compute the ground state solution and dynamics of GPE, and Cerimele, Pistella, and Succi [12] proposed a particle-inspired scheme. For the ground state solution of GPE, Edwards and Burnett presented a Runge–Kutta-type method and used it to solve one and three dimensions with spherical

---

†Department of Computational Science, National University of Singapore, Singapore 117543 (bao@cz3.nus.edu.sg, http://www.cz3.nus.edu.sg/~bao). The research of this author was supported by National University of Singapore grant R-151-000-027-112.

‡Department of Mathematics, Penn State University, University Park, PA 16802 (qdu@math.psu.edu, http://www.math.psu.edu/qdu). The research of this author was supported in part by NSF grant DMS-0196522.

symmetry time-independent GPE [19]. Adhikari [1] used this approach to get the ground state solution of GPE in two dimensions with radial symmetry. Bao and Tang [6] proposed a method by directly minimizing the energy functional. Other approaches include an explicit imaginary-time algorithm used by Chiofalo, Succi, and Tosi [13], a direct inversion in the iterated subspace (DIIS) used by Schneider and Feder [34], and a simple analytical-type method proposed by Dodd [17]. In fact, one of the fundamental problems in numerical simulation of BEC lies in computing the ground state solution.

We consider the NLS equation [7, 36]

$$i \, \psi_t = -\frac{1}{2} \, \Delta\psi + V(\mathbf{x}) \, \psi + \beta|\psi|^2\psi, \quad t > 0, \ \mathbf{x} \in \Omega \subseteq \mathbb{R}^d, \tag{1.1}$$

$$\psi(\mathbf{x}, t) = 0, \quad \mathbf{x} \in \Gamma = \partial\Omega, \ t \ge 0, \tag{1.2}$$

where Ω is a subset of $\mathbb{R}^d$ and $V(\mathbf{x})$ is a real-valued potential whose shape is determined by the type of system under investigation, and β positive/negative corresponds to the defocusing/focusing NLS equation. Equation (1.1) is known in BEC as the Gross–Pitaevskii equation [23, 31], where ψ is the macroscopic wave function of the condensate, t is time, $\mathbf{x}$ is the spatial coordinate, and $V(\mathbf{x})$ is a trapping potential, which usually is harmonic and can thus be written as $V(\mathbf{x}) = \frac{1}{2}(\gamma_1^2 x_1^2 + \cdots + \gamma_d^2 x_d^2)$ with $\gamma_1, \ldots, \gamma_d > 0$. Two important invariants of (1.1) are the *normalization of the wave function*

$$N(\psi) = \int_\Omega |\psi(\mathbf{x}, t)|^2 \, d\mathbf{x} = 1, \quad t \ge 0, \tag{1.3}$$

and the *energy*

$$E_\beta(\psi) = \int_\Omega \left[\frac{1}{2}|\nabla\psi(\mathbf{x}, t)|^2 + V(\mathbf{x})|\psi(\mathbf{x}, t)|^2 + \frac{\beta}{2}|\psi(\mathbf{x}, t)|^4\right] d\mathbf{x}, \quad t \ge 0. \tag{1.4}$$

To find a stationary solution of (1.1), we write

$$\psi(\mathbf{x}, t) = e^{-i\mu t}\phi(\mathbf{x}), \tag{1.5}$$

where μ is the chemical potential of the condensate and ϕ is a real function independent of time. Inserting into (1.1) gives the equation

$$\mu \, \phi(\mathbf{x}) = -\frac{1}{2}\Delta\phi(\mathbf{x}) + V(\mathbf{x}) \, \phi(\mathbf{x}) + \beta|\phi(\mathbf{x})|^2\phi(\mathbf{x}), \quad \mathbf{x} \in \Omega, \tag{1.6}$$

$$\phi(\mathbf{x}) = 0, \quad \mathbf{x} \in \Gamma, \tag{1.7}$$

for $\phi(\mathbf{x})$ under the normalization condition

$$\int_\Omega |\phi(\mathbf{x})|^2 d\mathbf{x} = 1. \tag{1.8}$$

This is a nonlinear eigenvalue problem under a constraint, and any eigenvalue μ can be computed from its corresponding eigenfunction ϕ by

$$\mu = \mu_\beta(\phi) = \int_\Omega \left[\frac{1}{2}|\nabla\phi(\mathbf{x})|^2 + V(\mathbf{x})|\phi(\mathbf{x})|^2 + \beta|\phi(\mathbf{x})|^4\right] d\mathbf{x}$$

$$= E_\beta(\phi) + \int_\Omega \frac{\beta}{2}|\phi(\mathbf{x})|^4 d\mathbf{x}. \tag{1.9}$$

The nonrotating BEC ground state solution $\phi_g(\mathbf{x})$ is a real nonnegative function found by minimizing the energy $E_\beta(\phi)$ under the constraint (1.8) [28]. In the physics literature (see, for instance, [2, 11, 13]), this minimizer was obtained by applying an imaginary time (i.e., $t \to -it$) in (1.1) and evolving a gradient flow with discrete normalization (GFDN) (see details in (2.1)–(2.3)). In fact, it is easy to show that the minimizer of $E_\beta(\phi)$ under the constraint (1.8) is an eigenfunction of (1.6).

The aim of this paper is to present a continuous normalized gradient flow (CNGF), prove its energy diminishing, and propose two new numerical methods to discretize the CNGF. This gives a mathematical justification of the imaginary time method, which is widely used in the physics literature to compute the ground state solution of BEC. Energy diminishing of the discretization of the CNGF is also proven. Extensive numerical results are reported to demonstrate the effectiveness of our new methods.

The paper is organized as follows. In section 2 we present the CNGF and prove energy diminishing of it and its discretized version. In section 3 we propose two numerical discretizations for the CNGF. In section 4 numerical comparison between the two methods and existing methods, as well as applications of the two methods for one-, two-, and three-dimensional ground state solutions of BEC, are reported. Finally in section 5 some conclusions are drawn. Throughout we adopt the standard notation for Sobolev spaces.

2. Normalized gradient flow and energy diminishing. In this section, we present the CNGF, prove its energy diminishing, and propose its semidiscretization.

2.1. Gradient flow with discrete normalization (GFDN). Various algorithms for computing the minimizer of the energy functional $E_\beta(\phi)$ under the constraint (1.8) have been studied in the literature. For instance, second order in time discretization scheme that preserves the normalization and energy diminishing properties were presented in [2, 18]. Perhaps one of the more popular techniques for dealing with the normalization constraint (1.8) is through the following construction: choose a time sequence $0 = t_0 < t_1 < t_2 < \cdots < t_n < \cdots$ with $\Delta t_n = t_{n+1} - t_n > 0$ and $k = \max_{n \geq 0} \Delta t_n$. To adapt an algorithm for the solution of the usual gradient flow to the minimization problem under a constraint, it is natural to consider the following splitting (or projection) scheme, which was widely used in the physics literature [11, 13, 18] for computing the ground state solution of BECs:

$$(2.1) \quad \phi_t = -\frac{1}{2}\frac{\delta E_\beta(\phi)}{\delta \phi} = \frac{1}{2}\Delta\phi - V(\mathbf{x})\phi - \beta\,|\phi|^2\phi, \quad \mathbf{x} \in \Omega,\ t_n < t < t_{n+1},\ n \geq 0,$$

$$(2.2) \quad \phi(x, t_{n+1}) \overset{\triangle}{=} \phi(\mathbf{x}, t_{n+1}^+) = \frac{\phi(\mathbf{x}, t_{n+1}^-)}{\|\phi(\cdot, t_{n+1}^-)\|}, \quad \mathbf{x} \in \Omega,\ n \geq 0,$$

$$(2.3) \quad \phi(\mathbf{x}, t) = 0, \quad \mathbf{x} \in \Gamma, \qquad \phi(\mathbf{x}, 0) = \phi_0(\mathbf{x}), \quad \mathbf{x} \in \Omega,$$

where $\phi(\mathbf{x}, t_n^\pm) = \lim_{t \to t_n^\pm} \phi(\mathbf{x}, t)$ and $\|\phi_0\| = 1$. Here we adopt the norm by $\| \cdot \| = \| \cdot \|_{L^2(\Omega)}$ and denote $\| \cdot \|_{L^m} = \| \cdot \|_{L^m(\Omega)}$ with m an integer. In fact, the gradient flow (2.1) can be viewed as applying the steepest decent method to the energy functional $E_\beta(\phi)$ without constraint, and (2.2) then projects the solution back to the unit sphere in order to satisfy the constraint (1.8). From the numerical point of view, the gradient flow (2.1) can be solved via traditional techniques, and the normalization of the gradient flow is simply achieved by a projection at the end of each time step.

2.2. Energy diminishing. Let

$$(2.4) \qquad \tilde{\phi}(\cdot, t) = \frac{\phi(\cdot, t)}{\|\phi(\cdot, t)\|}, \quad t_n \le t \le t_{n+1}, \ n \ge 0.$$

For the gradient flow (2.1), it is easy to establish the following basic facts.

LEMMA 2.1. *Suppose $V(\mathbf{x}) \ge 0$ for all $\mathbf{x} \in \Omega$, $\beta \ge 0$ and $\|\phi_0\| = 1$. Then*
  (i) $\|\phi(\cdot, t)\| \le \|\phi(\cdot, t_n)\| = 1$ for $t_n \le t \le t_{n+1}$, $n \ge 0$;
  (ii) *for any $\beta \ge 0$,*

$$(2.5) \qquad E_\beta(\phi(\cdot, t)) \le E_\beta(\phi(\cdot, t')), \quad t_n \le t' < t \le t_{n+1}, \ n \ge 0;$$

  (iii) *for $\beta = 0$,*

$$(2.6) \qquad E_0(\tilde{\phi}(\cdot, t)) \le E_0(\tilde{\phi}(\cdot, t_n)), \quad t_n \le t \le t_{n+1}, \ n \ge 0.$$

Proof. (i) and (ii) follow the standard techniques used for gradient flow. As for (iii), from (1.4) with $\psi = \tilde{\phi}$ and $\beta = 0$, (2.1), (2.3), and (2.4), integration by parts, and the Schwartz inequality, we obtain

$$\frac{d}{dt} E_0(\tilde{\phi}) = \frac{d}{dt} \int_\Omega \left[\frac{|\nabla \phi|^2}{2\|\phi\|^2} + \frac{V(\mathbf{x})\phi^2}{\|\phi\|^2} \right] d\mathbf{x}$$

$$= 2 \int_\Omega \left[\frac{\nabla \phi \cdot \nabla \phi_t}{2\|\phi\|^2} + \frac{V(\mathbf{x})\phi \, \phi_t}{\|\phi\|^2} \right] d\mathbf{x} - \left(\frac{d}{dt}\|\phi\|^2 \right) \int_\Omega \left[\frac{|\nabla \phi|^2}{2\|\phi\|^4} + \frac{V(\mathbf{x})\phi^2}{\|\phi\|^4} \right] d\mathbf{x}$$

$$(2.7) \qquad = 2 \int_\Omega \frac{\left[-\frac{1}{2}\Delta\phi + V(\mathbf{x})\phi \right] \phi_t}{\|\phi\|^2} d\mathbf{x} - \left(\frac{d}{dt}\|\phi\|^2 \right) \int_\Omega \frac{\frac{1}{2}|\nabla \phi|^2 + V(\mathbf{x})\phi^2}{\|\phi\|^4} d\mathbf{x}$$

$$= -2\frac{\|\phi_t\|^2}{\|\phi\|^2} + \frac{1}{2\|\phi\|^4}\left(\frac{d}{dt}\|\phi\|^2 \right)^2 = \frac{2}{\|\phi\|^4}\left[\left(\int_\Omega \phi \, \phi_t d\mathbf{x} \right)^2 - \|\phi\|^2\|\phi_t\|^2 \right]$$

$$\le 0, \quad t_n \le t \le t_{n+1}.$$

This implies (2.6). □

Remark 2.2. The property (2.5) is often referred to as the energy diminishing property of the gradient flow. It is interesting to note that (2.6) implies that the energy diminishing property is preserved even with the normalization of the solution of the gradient flow for $\beta = 0$, that is, for linear evolution equations.

Remark 2.3. When $\beta > 0$, the solution of (2.1)–(2.3) may not preserve the normalized energy diminishing property

$$E_\beta(\tilde{\phi}(\cdot, t)) \le E_\beta(\tilde{\phi}(\cdot, t')), \quad 0 \le t' < t \le t_1,$$

for any $t_1 > 0$. In fact, we solve (2.1), (2.3) in one dimension with $\Omega = \mathbb{R}$, $t_1 = 2$ and $V(x) = x^2/2$ numerically by the time-splitting spectral method (see details in the next section) for the initial condition $\phi_0(x) = (\pi/2)^{-1/4} e^{-x^2}$. Figure 2.1 shows, for different β, the energy $E_\beta(\tilde{\phi}(\cdot, t)) = E_\beta(\phi(\cdot, t)/\|\phi(\cdot, t)\|)$ under mesh size $h = 1/32$ and time step $k = 0.0001$. From the figure, we can see $E_\beta(\tilde{\phi})$ diminishing for $0 \le t < \infty$ when $\beta = 0$. But when $\beta > 0$, we have $E_\beta(\tilde{\phi})$ diminishing only for $0 \le t \le t_*$ with some finite $t_* < \infty$.

From Lemma 2.1, we immediately get the following.

THEOREM 2.4. *Suppose $V(\mathbf{x}) \ge 0$ for all $\mathbf{x} \in \Omega$ and $\|\phi_0\| = 1$. For $\beta = 0$, GFDN (2.1)–(2.3) is energy diminishing for any time step k and initial data ϕ_0, i.e.,*

$$(2.8) \quad E_0(\phi(\cdot, t_{n+1})) \le E_0(\phi(\cdot, t_n)) \le \cdots \le E_0(\phi(\cdot, 0)) = E_0(\phi_0), \quad n = 0, 1, 2, \dots.$$
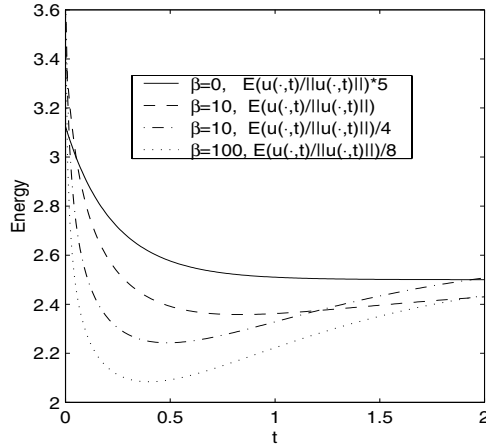
FIG. 2.1. $E_\beta(\tilde\phi)$ (labeled $E(u/\|u\|)$) as a function of time in Remark 2.3 for different β.

2.3. Continuous normalized gradient flow (CNGF). In fact, the normalized step (2.2) is equivalent to solving the following ODE *exactly*:

$$(2.9) \qquad \phi_t(\mathbf{x}, t) = \mu_\phi(t, k)\phi(\mathbf{x}, t), \quad \mathbf{x} \in \Omega, \ t_n < t < t_{n+1}, \ n \geq 0,$$

$$(2.10) \qquad \phi(\mathbf{x}, t_n^+) = \phi(\mathbf{x}, t_{n+1}^-), \quad \mathbf{x} \in \Omega,$$

where

$$(2.11) \qquad \mu_\phi(t, k) \equiv \mu_\phi(t_{n+1}, \Delta t_n) = -\frac{1}{2\,\Delta t_n} \ln \|\phi(\cdot, t_{n+1}^-)\|^2, \quad t_n \leq t \leq t_{n+1}.$$

Thus the GFDN (2.1)–(2.3) can be viewed as a first-order splitting method for the gradient flow with discontinuous coefficients:

$$(2.12) \qquad \phi_t = \frac{1}{2}\Delta\phi - V(\mathbf{x})\phi - \beta\,|\phi|^2\phi + \mu_\phi(t, k)\phi, \quad \mathbf{x} \in \Omega, \ t \geq 0,$$

$$(2.13) \qquad \phi(\mathbf{x}, t) = 0, \quad \mathbf{x} \in \Gamma, \qquad \phi(\mathbf{x}, 0) = \phi_0(\mathbf{x}), \quad \mathbf{x} \in \Omega.$$

Letting $k \to 0$, we see that

$$(2.14)$$
$$\lim_{k\to 0^+} \mu_\phi(t, k) = \mu_\phi(t) = \frac{1}{\|\phi(\cdot, t)\|^2} \int_\Omega \left[\frac{1}{2}|\nabla\phi(\mathbf{x}, t)|^2 + V(\mathbf{x})\phi^2(\mathbf{x}, t) + \beta\phi^4(\mathbf{x}, t)\right] d\mathbf{x}.$$

This suggests that we should consider the following CNGF:

$$(2.15) \qquad \phi_t = \frac{1}{2}\Delta\phi - V(\mathbf{x})\phi - \beta\,|\phi|^2\phi + \mu_\phi(t)\phi, \quad \mathbf{x} \in \Omega, \ t \geq 0,$$

$$(2.16) \qquad \phi(\mathbf{x}, t) = 0, \quad \mathbf{x} \in \Gamma, \qquad \phi(\mathbf{x}, 0) = \phi_0(\mathbf{x}), \quad \mathbf{x} \in \Omega.$$

In fact, the right-hand side of (2.15) is the same as (1.6) if we view $\mu_\phi(t)$ as a Lagrange multiplier for the constraint (1.8). Furthermore for the above CNGF, as observed in [2, 18], the solution of (2.15) also satisfies the following theorem.

THEOREM 2.5. *Suppose $V(\mathbf{x}) \geq 0$ for all $\mathbf{x} \in \Omega$, $\beta \geq 0$ and $\|\phi_0\| = 1$. Then the CNGF (2.15)–(2.16) is normalization conservation and energy diminishing, i.e.,*

$$(2.17) \qquad \|\phi(\cdot, t)\|^2 = \int_\Omega \phi^2(\mathbf{x}, t) d\mathbf{x} = \|\phi_0\|^2 = 1, \quad t \geq 0,$$

$$(2.18) \qquad \frac{d}{dt} E_\beta(\phi) = -2\|\phi_t(\cdot, t)\|^2 \leq 0, \quad t \geq 0,$$

which in turn implies

$$E_\beta(\phi(\cdot, t_1)) \geq E_\beta(\phi(\cdot, t_2)), \quad 0 \leq t_1 \leq t_2 < \infty.$$

Remark 2.6. We see from the above theorem that the energy diminishing property is preserved in the continuous dynamic system (2.15).

Using an argument similar to that in [29, 35], we may also get that as $t \to \infty$, ϕ approaches to a steady state solution, which is a critical point of the energy. In nonrotating BECs, it has a unique real-valued nonnegative ground state solution $\phi_g(\mathbf{x}) \geq 0$ for all $\mathbf{x} \in \Omega$ [28]. We choose the initial data $\phi_0(\mathbf{x}) \geq 0$ for $\mathbf{x} \in \Omega$, e.g., the ground state solution of the linear Schrödinger equation with a harmonic oscillator potential [6, 7]. Under this kind of initial data, the ground state solution ϕ_g and its corresponding chemical potential μ_g can be obtained from the steady state solution of the CNGF (2.15)–(2.16), i.e.,

$$(2.19) \quad \phi_g(\mathbf{x}) = \lim_{t \to \infty} \phi(\mathbf{x}, t), \quad \mathbf{x} \in \Omega, \qquad \mu_g = \mu_\beta(\phi_g) = E_\beta(\phi_g) + \frac{\beta}{2} \int_\Omega \phi_g^4(\mathbf{x}) d\mathbf{x}.$$

2.4. Semi-implicit time discretization. To further discretize (2.1), we here consider the following semi-implicit time discretization scheme:

$$(2.20) \qquad \frac{\tilde{\phi}^{n+1} - \phi^n}{k} = \frac{1}{2} \Delta \tilde{\phi}^{n+1} - V(\mathbf{x}) \tilde{\phi}^{n+1} - \beta |\phi^n|^2 \tilde{\phi}^{n+1}, \quad \mathbf{x} \in \Omega,$$

$$(2.21) \qquad \tilde{\phi}^{n+1}(\mathbf{x}) = 0, \quad \mathbf{x} \in \Gamma, \qquad \phi^{n+1}(\mathbf{x}) = \tilde{\phi}^{n+1}(\mathbf{x})/\|\tilde{\phi}^{n+1}\|, \quad \mathbf{x} \in \Omega.$$

Notice that since (2.20) becomes linear, the solution at the new time step becomes relatively simple. In other words, in each discrete time interval, we may view (2.20) as a discretization of a linear gradient flow with a modified potential $\tilde{V}_n(\mathbf{x}) = V(\mathbf{x}) + \beta|\phi^n(\mathbf{x})|^2$.

We now first present the following lemma.

LEMMA 2.7. *Suppose $\beta \geq 0$ and $V(\mathbf{x}) \geq 0$ for all $\mathbf{x} \in \Omega$ and $\|\phi^n\| = 1$. Then*

$$(2.22) \qquad \int_\Omega |\tilde{\phi}^{n+1}|^2 d\mathbf{x} \leq \int_\Omega \phi^n \, \tilde{\phi}^{n+1} d\mathbf{x}, \qquad \int_\Omega |\tilde{\phi}^{n+1}|^4 d\mathbf{x} \leq \int_\Omega |\phi^n|^2 \, |\tilde{\phi}^{n+1}|^2 d\mathbf{x}.$$

Proof. Multiplying both sides of (2.20) by $\tilde{\phi}^{n+1}$, integrating over Ω, and applying integration by parts, we obtain

$$\int_\Omega (|\tilde{\phi}^{n+1}|^2 - \phi^n \tilde{\phi}^{n+1}) d\mathbf{x} = -k \int_\Omega \left[\frac{1}{2} |\nabla \tilde{\phi}^{n+1}|^2 + \tilde{V}_n(\mathbf{x}) |\tilde{\phi}^{n+1}|^2 \right] d\mathbf{x} \leq 0,$$

which leads to the first inequality in (2.22). Similarly,

$$
\begin{aligned}
\int_\Omega |\tilde{\phi}^{n+1}|^2 |\phi^n|^2 d\mathbf{x} &= \int_\Omega |\tilde{\phi}^{n+1}|^2 \left| \tilde{\phi}^{n+1} - \frac{k}{2}\Delta\tilde{\phi}^{n+1} + k\tilde{V}_n(\mathbf{x})\tilde{\phi}^{n+1} \right|^2 d\mathbf{x} \\
&= \int_\Omega |\tilde{\phi}^{n+1}|^2 \left[|\tilde{\phi}^{n+1}|^2 - 2\frac{k}{2}\tilde{\phi}^{n+1}\Delta\tilde{\phi}^{n+1} + 2k\tilde{V}_n(\mathbf{x})|\tilde{\phi}^{n+1}|^2 \right] d\mathbf{x} \\
&\quad + \int_\Omega |\tilde{\phi}^{n+1}|^2 \left| \frac{k}{2}\Delta\tilde{\phi}^{n+1} - k\tilde{V}_n(\mathbf{x})\tilde{\phi}^{n+1} \right|^2 d\mathbf{x} \\
&= \int_\Omega |\tilde{\phi}^{n+1}|^2 \left[|\tilde{\phi}^{n+1}|^2 + 3k|\nabla\tilde{\phi}^{n+1}|^2 + 2k\tilde{V}_n(\mathbf{x})|\tilde{\phi}^{n+1}|^2 \right] d\mathbf{x} \\
&\quad + \int_\Omega |\tilde{\phi}^{n+1}|^2 \left| \frac{k}{2}\Delta\tilde{\phi}^{n+1} - k\tilde{V}_n(\mathbf{x})\tilde{\phi}^{n+1} \right|^2 d\mathbf{x} \\
&\geq \int_\Omega |\tilde{\phi}^{n+1}|^4 d\mathbf{x}.
\end{aligned}
\tag{2.23}
$$

This implies the second inequality in (2.22). $\square$

Given a linear self-adjoint operator A in a Hilbert space H with inner product $(\cdot, \cdot)$, and assuming that A is positive definite in the sense that for some positive constant c, $(u, Au) \geq c(u, u)$ for any $u \in H$. We now present a simple lemma.

LEMMA 2.8. *For any $k > 0$, and $(I + kA)u = v$, we have*

$$
\frac{(u, Au)}{(u, u)} \leq \frac{(v, Av)}{(v, v)}.
\tag{2.24}
$$

Proof. Since A is self-adjoint and positive definite, by the Hölder inequality, we have for any $p, q \geq 1$ with $p + q = pq$ that

$$
(u, Au) \leq (u, u)^{1/p}(u, A^q u)^{1/q},
$$

which leads to

$$
(u, Au) \leq (u, u)^{1/2}(u, A^2 u)^{1/2}, \qquad (u, Au)(u, A^2 u) \leq (u, u)(u, A^3 u).
$$

Direct calculation then gives

$$
\begin{aligned}
(u, Au)&((I + kA)u, (I + kA)u) \\
&= (u, Au)(u, u) + 2k(u, Au)^2 + k^2(u, Au)(u, A^2 u) \\
&\leq (u, Au)(u, u) + 2k(u, u)(u, A^2 u) + k^2(u, u)(u, A^3 u) \\
&= (u, u)((I + kA)u, A(I + kA)u). \qquad \square
\end{aligned}
\tag{2.25}
$$

Let us define a modified energy $\tilde{E}_{\phi^n}$ as

$$
\tilde{E}_{\phi^n}(u) = \int_\Omega \left[\frac{1}{2}|\nabla u|^2 + \tilde{V}_n(\mathbf{x})|u|^2 \right] d\mathbf{x} = \int_\Omega \left[\frac{1}{2}|\nabla u|^2 + V(\mathbf{x})|u|^2 + \beta|\phi^n|^2|u|^2 \right] d\mathbf{x};
$$

we then get the following from the above lemma.

LEMMA 2.9. *Suppose $V(\mathbf{x}) \geq 0$ for all $\mathbf{x} \in \Omega$, $\beta \geq 0$ and $\|\phi^n\| = 1$. Then*

$$
\tilde{E}_{\phi^n}(\tilde{\phi}^{n+1}) \leq \frac{\tilde{E}_{\phi^n}(\tilde{\phi}^{n+1})}{\|\tilde{\phi}^{n+1}\|} = \tilde{E}_{\phi^n}\left(\frac{\tilde{\phi}^{n+1}}{\|\tilde{\phi}^{n+1}\|} \right) = \tilde{E}_{\phi^n}(\phi^{n+1}) \leq \tilde{E}_{\phi^n}(\phi_n).
\tag{2.26}
$$

Using the inequality (2.22), we in turn get the following lemma.

LEMMA 2.10. *Suppose $V(\mathbf{x}) \geq 0$ for all $\mathbf{x} \in \Omega$ and $\beta \geq 0$. Then*

$$\tilde{E}_\beta(\tilde{\phi}^{n+1}) \leq \tilde{E}_\beta(\phi^n),$$

where

$$\tilde{E}_\beta(u) = \int_\Omega \left[\frac{1}{2}|\nabla u|^2 + V(\mathbf{x})|u|^2 + \beta|u|^4\right] d\mathbf{x}.$$

Remark 2.11. As we noted earlier, for $\beta = 0$, the energy diminishing property is preserved in the GFDN (2.1)–(2.3) and semi-implicit time discretization (2.20)–(2.21). For $\beta > 0$, the energy diminishing property in general does *not* hold uniformly for all ϕ_0 and all step sizes $k > 0$; a justification on the energy diminishing is presently only possible for a modified energy within two adjacent steps.

2.5. Discretized normalized gradient flow (DNGF). Consider a discretization for the GFDN (2.20)–(2.21) (or a full discretization of (2.15)–(2.16)),

$$(2.27) \qquad \frac{\tilde{U}^{n+1} - U^n}{k} = -A\tilde{U}^{n+1}, \quad U^{n+1} = \frac{\tilde{U}^{n+1}}{\|\tilde{U}^{n+1}\|}, \quad n = 0, 1, 2, \dots,$$

where $U^n = (u_1^n, u_2^n, \dots, u_{M-1}^n)^T$, $k > 0$, is time step and A is an $(M-1) \times (M-1)$ symmetric positive definite matrix. We adopt the inner product, norm, and energy of vectors $U = (u_1, u_2, \dots, u_{M-1})^T$ and $V = (v_1, v_2, \dots, v_{M-1})^T$ as

(2.28)

$$(U, V) = U^T V = \sum_{j=1}^{M-1} u_j\, v_j, \quad \|U\|^2 = U^T U = (U, U), \quad E_0(U) = U^T A U = (U, AU),$$

respectively. Using the finite-dimensional version of the lemmas given in the previous subsection, we have the following.

THEOREM 2.12. *Suppose $\|U^0\| = 1$ and A is symmetric positive definite. Then the DNGF (2.27) is energy diminishing, i.e.,*

$$(2.29) \qquad E_0(U^{n+1}) \leq E_0(U^n) \leq \cdots \leq E_0(U^0), \quad n = 0, 1, 2, \dots.$$

Furthermore if $I + kA$ is an M-matrix [21], then $(I + kA)^{-1}$ is a nonnegative matrix (i.e., with nonnegative entries). Thus the flow is monotone; i.e., if U^0 is a nonnegative vector, then U^n is also a nonnegative vector for all $n \geq 0$.

Remark 2.13. If a discretization for the GFDN (2.20)–(2.21) reads

$$(2.30) \qquad \frac{\tilde{U}^{n+1} - U^n}{k} = -BU^n, \quad U^{n+1} = \frac{\tilde{U}^{n+1}}{\|\tilde{U}^{n+1}\|}, \quad n = 0, 1, 2, \dots,$$

for some symmetric, positive definite B with $\rho(kB) < 1$ ($\rho(B)$ being the spectral radius of B), then (2.29) is satisfied by choosing

$$A = \frac{1}{k}((I - kB)^{-1} - I) = (I - kB)^{-1}B.$$

Remark 2.14. If a discretization for the GFDN (2.20)–(2.21) reads

$$(2.31) \qquad \tilde{U}^{n+1} = BU^n, \quad U^{n+1} = \frac{\tilde{U}^{n+1}}{\|\tilde{U}^{n+1}\|}, \quad n = 0, 1, 2, \dots,$$

for some symmetric, positive definite B with $\rho(B) < 1$, then (2.29) is satisfied by choosing

$$A = \frac{1}{k}(B^{-1} - I).$$

Remark 2.15. If a discretization for the GFDN (2.20)–(2.21) reads

$$(2.32) \qquad \frac{\tilde{U}^{n+1} - U^n}{k} = -B\tilde{U}^{n+1} - CU^n, \quad U^{n+1} = \frac{\tilde{U}^{n+1}}{\|\tilde{U}^{n+1}\|}, \quad n = 0, 1, 2, \dots ,$$

for some symmetric, positive definite B and C with $\rho(kC) < 1$, then (2.29) is satisfied by choosing

$$A = (I - kC)^{-1}(B + C).$$

3. Numerical methods and energy diminishing. In this section, we will present two numerical methods to discretize the GFDN (2.1)–(2.3) (or a full discretization of the CNGF (2.15)–(2.16)). For simplicity of notation we introduce the methods for the case of one spatial dimension $(d = 1)$ with homogeneous Dirichlet boundary conditions. Generalizations to higher dimension are straightforward for tensor product grids, and the results remain valid without modifications. For $d = 1$, we have

$$(3.1) \qquad \phi_t = \frac{1}{2}\phi_{xx} - V(x)\phi - \beta\,|\phi|^2\phi, \quad x \in \Omega = (a, b),\ t_n < t < t_{n+1},\ n \geq 0,$$

$$(3.2) \qquad \phi(x, t_{n+1}) \overset{\triangle}{=} \phi(x, t_{n+1}^+) = \frac{\phi(x, t_{n+1}^-)}{\|\phi(\cdot, t_{n+1}^-)\|}, \qquad a \leq x \leq b, \quad n \geq 0,$$

$$(3.3) \qquad \phi(x, 0) = \phi_0(x), \quad a \leq x \leq b, \qquad \phi(a, t) = \phi(b, t) = 0, \quad t \geq 0,$$

with

$$\|\phi_0\|^2 = \int_a^b \phi_0^2(x)\ dx = 1.$$

3.1. Numerical methods. We choose the spatial mesh size $h = \Delta x > 0$ with $h = (b - a)/M$ and M an even positive integer; the time step is given by $k = \Delta t > 0$, and we define grid points and time steps by

$$x_j := a + j\,h, \quad t_n := n\,k, \quad j = 0, 1, \dots, M,\ n = 0, 1, 2, \dots .$$

Let ϕ_j^n be the numerical approximation of $\phi(x_j, t_n)$ and ϕ^n the solution vector at time $t = t_n = nk$ with components ϕ_j^n.

Backward Euler finite difference (BEFD). We use backward Euler for time discretization and second-order centered finite difference for spatial derivatives. The detail scheme is

$$\frac{\phi_j^* - \phi_j^n}{k} = \frac{1}{2h^2}[\phi_{j+1}^* - 2\phi_j^* + \phi_{j-1}^*] - V(x_j)\phi_j^* - \beta(\phi_j^n)^2\phi_j^*, \quad j = 1, \dots, M - 1,$$

$$(3.4) \qquad\qquad \phi_0^* = \phi_M^* = 0, \qquad \phi_j^0 = \phi_0(x_j), \quad j = 0, 1, \dots, M,$$

$$\phi_j^{n+1} = \frac{\phi_j^*}{\|\phi^*\|}, \quad j = 0, \dots, M,\ n = 0, 1, \dots ,$$

where the norm is defined as $\|\phi^*\|^2 = h\sum_{j=1}^{M-1}(\phi_j^*)^2$.

Time-splitting sine-spectral method (TSSP). From time $t = t_n$ to time $t = t_{n+1}$, the equation (3.1) is solved in two steps. First, one solves

$$(3.5) \qquad \qquad \phi_t = \frac{1}{2}\phi_{xx}$$

for one time step of length k, followed by solving

$$(3.6) \qquad \phi_t(x,t) = -V(x)\phi(x,t) - \beta|\phi|^2\phi(x,t), \quad t_n \le t \le t_{n+1},$$

again for the same time step. Equation (3.5) is discretized in space by the sine-spectral method and integrated in time *exactly*. For $t \in [t_n, t_{n+1}]$, multiplying the ODE (3.6) by $\phi(x,t)$, one obtains with $\rho(x,t) = \phi^2(x,t)$

$$(3.7) \qquad \rho_t(x,t) = -2V(x)\rho(x,t) - 2\beta\rho^2(x,t), \quad t_n \le t \le t_{n+1}.$$

The solution of the ODE (3.7) can be expressed as

$$(3.8) \qquad \rho(x,t) = \begin{cases} \dfrac{V(x)\rho(x,t_n)}{(V(x) + \beta\rho(x,t_n))e^{2V(x)(t-t_n)} - \beta\rho(x,t_n)}, & V(x) \ne 0, \\[2em] \dfrac{\rho(x,t_n)}{1 + 2\beta\rho(x,t_n)(t - t_n)}, & V(x) = 0. \end{cases}$$

Combining the splitting step via the standard second-order Strang splitting for solving the GFDN (3.1)–(3.3), in detail, the steps for obtaining ϕ_j^{n+1} from ϕ_j^n are given by

$$(3.9) \quad \begin{aligned} \phi_j^* &= \begin{cases} \sqrt{\dfrac{V(x_j)e^{-kV(x_j)}}{V(x_j) + \beta(1 - e^{-kV(x_j)})|\phi_j^n|^2}} \; \phi_j^n, & V(x_j) \ne 0, \\[1.5em] \dfrac{1}{\sqrt{1 + \beta k|\phi_j^n|^2}} \; \phi_j^n, & V(x_j) = 0, \end{cases} \\[2em] \phi_j^{**} &= \sum_{l=1}^{M-1} e^{-k\mu_l^2/2} \; \widehat{\phi_l^*} \; \sin(\mu_l(x_j - a)), \quad j = 1, 2, \ldots, M - 1, \\[1.5em] \phi_j^{***} &= \begin{cases} \sqrt{\dfrac{V(x_j)e^{-kV(x_j)}}{V(x_j) + \beta(1 - e^{-kV(x_j)})|\phi_j^{**}|^2}} \; \phi_j^{**}, & V(x_j) \ne 0, \\[1.5em] \dfrac{1}{\sqrt{1 + \beta k|\phi_j^{**}|^2}} \; \phi_j^{**}, & V(x_j) = 0, \end{cases} \\[1.5em] \phi_j^{n+1} &= \dfrac{\phi_j^{***}}{\|\phi^{***}\|}, \quad j = 0, \ldots, M, \; n = 0, 1, \ldots, \end{aligned}$$

where $\widehat{U}_l$ are the sine-transform coefficients of a real vector $U = (u_0, u_1, \ldots, u_M)^T$ with $u_0 = u_M = 0$, which are defined as

$$(3.10) \qquad \mu_l = \frac{\pi l}{b - a}, \quad \widehat{U}_l = \frac{2}{M}\sum_{j=1}^{M-1} u_j \; \sin(\mu_l(x_j - a)), \quad l = 1, 2, \ldots, M - 1,$$

and

$$\phi_j^0 = \phi(x_j, 0) = \phi_0(x_j), \quad j = 0, 1, 2, \ldots, M.$$

Note that the only time discretization error of TSSP is the splitting error, which is second order in k.

For comparison purposes we review a few other numerical methods which are currently used for solving the GFDN (3.1)–(3.3). One is the Crank–Nicolson finite difference (CNFD) scheme [20]:

$$
\frac{\phi_j^* - \phi_j^n}{k} = \frac{1}{4h^2}[\phi_{j+1}^* - 2\phi_j^* + \phi_{j-1}^* + \phi_{j+1}^n - 2\phi_j^n + \phi_{j-1}^n]
$$

$$
- \frac{V(x_j)}{2}[\phi_j^* + \phi_j^n] - \frac{\beta|\phi_j^n|^2}{2}[\phi_j^* + \phi_j^n], \quad j = 1, \ldots, M-1,
$$

(3.11)
$$
\phi_0^* = \phi_M^* = 0, \qquad \phi_j^0 = \phi_0(x_j), \quad j = 0, 1, \ldots, M,
$$

$$
\phi_j^{n+1} = \frac{\phi_j^*}{\|\phi^*\|}, \quad j = 0, \ldots, M, \ n = 0, 1, \ldots .
$$

Another one is the forward Euler finite difference (FEFD) method [13]:

$$
\frac{\phi_j^* - \phi_j^n}{k} = \frac{1}{2h^2}[\phi_{j+1}^n - 2\phi_j^n + \phi_{j-1}^n] - V(x_j)\phi_j^n - \beta|\phi_j^n|^2\phi_j^n, \quad j = 1, \ldots, M-1,
$$

(3.12)
$$
\phi_0^* = \phi_M^* = 0, \quad \phi_j^0 = \phi_0(x_j), \quad j = 0, 1, \ldots, M,
$$

$$
\phi_j^{n+1} = \frac{\phi_j^*}{\|\phi^*\|}, \quad j = 0, \ldots, M, \ n = 0, 1, \ldots .
$$

3.2. Energy diminishing. First we analyze the energy diminishing of the different numerical methods for the linear case, i.e., $\beta = 0$ in (3.1). We introduce the following notation:

$$
\Phi^n = (\phi_1^n, \phi_2^n, \ldots, \phi_{M-1}^n)^T,
$$

$$
D = (d_{jl})_{(M-1)\times(M-1)}, \quad \text{with } d_{jl} = \frac{1}{2h^2}
\begin{cases}
2, & j = l, \\
-1, & |j - l| = -1, \quad j, l = 1, \ldots, M-1, \\
0, & \text{otherwise},
\end{cases}
$$

$$
E = \text{diag}(V(x_1), V(x_2), \ldots, V(x_{M-1})),
$$
$$
F(\Phi) = \text{diag}(\phi_1^2, \phi_2^2, \ldots, \phi_{M-1}^2), \quad \text{with } \Phi = (\phi_1, \phi_2, \ldots, \phi_{M-1})^T,
$$

$$
G = (g_{jl})_{(M-1)\times(M-1)}, \quad \text{with } g_{jl} = \frac{2}{M}\sum_{m=1}^{M-1} \sin\frac{\pi m j}{M} \sin\frac{\pi m l}{M} e^{-k\mu_m^2/2},
$$

$$
H = \text{diag}(e^{-kV(x_1)/2}, e^{-kV(x_2)/2}, \ldots, e^{-kV(x_{M-1})/2}).
$$

Then the BEFD discretization (3.4) (called as BEFD normalized flow) with $\beta = 0$ can be expressed as

(3.13)
$$
\frac{\Phi^* - \Phi^n}{k} = -(D + E)\Phi^*, \quad \Phi^{n+1} = \frac{\Phi^*}{\|\Phi^*\|}, \quad n = 0, 1, \ldots .
$$

The TSSP discretization (3.9) (called the TSSP normalized flow) with $\beta = 0$ can be expressed as

(3.14)
$$
\Phi^{***} = H\Phi^{**} = HG\Phi^* = HGH\Phi^n, \quad \Phi^{n+1} = \frac{\Phi^*}{\|\Phi^*\|}, \quad n = 0, 1, \ldots .
$$

The CNFD discretization (3.11) (called the CNFD normalized flow) with $\beta = 0$ can be expressed as

$$(3.15) \quad \frac{\Phi^* - \Phi^n}{k} = -\frac{1}{2}(D+E)\Phi^* - \frac{1}{2}(D+E)\Phi^n, \quad \Phi^{n+1} = \frac{\Phi^*}{\|\Phi^*\|}, \quad n = 0, 1, \ldots.$$

The FEFD discretization (3.12) (called the FEFD normalized flow) with $\beta = 0$ can be expressed as

$$(3.16) \quad \frac{\Phi^* - \Phi^n}{k} = -(D+E)\Phi^n, \quad \Phi^{n+1} = \frac{\Phi^*}{\|\Phi^*\|}, \quad n = 0, 1, \ldots.$$

It is easy to see that D and G are symmetric positive definite matrices. Furthermore D is also an M-matrix and $\rho(D) = (1 + \cos\frac{\pi}{M})/h^2 < 2/h^2$ and $\rho(G) = e^{-k\mu_1^2/2} < 1$. Applying Theorem 2.12 and Remarks 2.13, 2.14, and 2.15, we have the following.

THEOREM 3.1. *Suppose $V \geq 0$ in Ω and $\beta = 0$. We have that*

(i) *the BEFD normalized flow (3.4) is energy diminishing and monotone for any $k > 0$;*

(ii) *the TSSP normalized flow (3.9) is energy diminishing for any $k > 0$;*

(iii) *the CNFD normalized flow (3.11) is energy diminishing and monotone provided that*

$$(3.17) \quad k \leq \frac{2}{2/h^2 + \max_j V(x_j)} = \frac{2h^2}{2 + h^2 \max_j V(x_j)};$$

(iv) *the FEFD normalized flow (3.12) is energy diminishing and monotone provided that*

$$(3.18) \quad k \leq \frac{1}{2/h^2 + \max_j V(x_j)} = \frac{h^2}{2 + h^2 \max_j V(x_j)}.$$

For the nonlinear case, i.e., $\beta > 0$, we analyze only the *energy* between two steps of the BEFD flow (3.4). In this case, consider

$$(3.19) \quad \frac{\tilde{\Phi}^{n+1} - \Phi^n}{k} = -(D + E + \beta F(\Phi^n))\tilde{\Phi}^{n+1}, \quad \Phi^{n+1} = \frac{\tilde{\Phi}^{n+1}}{\|\tilde{\Phi}^{n+1}\|}.$$

LEMMA 3.2. *Suppose $V \geq 0$, $\beta > 0$, and $\|\Phi^n\| = 1$. Then for the flow (3.19), we have*

$$(3.20) \quad \tilde{E}_\beta(\tilde{\Phi}^{n+1}) \leq \tilde{E}_\beta(\Phi^n), \quad \tilde{E}_{\Phi^n}(\Phi^{n+1}) \leq \tilde{E}_{\Phi^n}(\Phi^n),$$

where

$$(3.21) \quad \tilde{E}_\beta(\Phi) = (\Phi, (D + E + \beta F(\Phi))\Phi) = \Phi^T(D+E)\Phi + \beta \sum_{j=1}^{M-1} \phi_j^4,$$

$$(3.22) \quad \tilde{E}_{\Phi^n}(\Phi) = (\Phi, (D + E + \beta F(\Phi^n))\Phi) = \Phi^T(D+E)\Phi + \beta \sum_{j=1}^{M-1} \phi_j^2(\phi_j^n)^2.$$

Proof. Combining (3.19), (2.27), and Theorem 2.12, we have

$$
\begin{aligned}
(\tilde{\Phi}^{n+1}, (D + E + \beta F(\Phi^n))\tilde{\Phi}^{n+1}) &\leq \frac{(\tilde{\Phi}^{n+1}, (D + E + \beta F(\Phi^n))\tilde{\Phi}^{n+1})}{(\tilde{\Phi}^{n+1}, \tilde{\Phi}^{n+1})} \\
&\leq \frac{(\Phi^n, (D + E + \beta F(\Phi^n))\Phi^n)}{(\Phi^n, \Phi^n)} = \tilde{E}_\beta(\Phi^n).
\end{aligned}
$$
(3.23)

Similar to the proof of (2.22), we have

$$
\sum_{j=1}^{M-1} (\phi_j^n)^2 (\tilde{\phi}_j^{n+1})^2 \geq \sum_{j=1}^{M-1} (\tilde{\phi}_j^{n+1})^4.
$$
(3.24)

The required result (3.20) is a combination of (3.24) and (3.23). □

4. Numerical results. We now compare the four different numerical discretizations for the CNGF and report numerical results of the ground state solutions of BECs in one, two, and three dimensions with magnetic trap confinement potential. We also compute the ground state solutions with the potential of a stirrer corresponding a far-blue detuned Gaussian laser beam and central vortex state by the methods BEFD or TSSP.

Due to the ground state solution $\phi_g(\mathbf{x}) \geq 0$ for $\mathbf{x} \in \Omega$ in nonrotating BEC [28], in our computations, the initial condition (2.3) is always chosen such that $\phi_0(\mathbf{x}) \geq 0$ and decays to zero sufficiently fast as $|\mathbf{x}| \to \infty$. We choose an appropriately large interval, rectangle, and box in one, two, and three dimensions, respectively, to avoid the homogeneous Dirichlet boundary condition (3.3) from introducing a significant (aliasing) error relative to the whole space problem. To quantify the ground state solution $\phi_g(\mathbf{x})$, we define the radius mean square

$$
\alpha_{\mathrm{rms}} = \|\alpha\phi_g\|_{L^2(\Omega)} = \sqrt{\int_\Omega \alpha^2 \phi_g^2(\mathbf{x}) d\mathbf{x}}, \quad \alpha = x, y, \text{ or } z.
$$
(4.1)

4.1. Comparisons of different methods.
Example 4.1. CNGF in one dimension, i.e., $d = 1$ in (2.15)–(2.16). We consider two cases:

I. *The linear case ($\beta = 0$) with a double-well potential,*

$$
V(x) = \frac{1}{2}(1 - x^2)^2, \quad \beta = 0, \quad \phi_0(x) = \frac{1}{(4\pi)^{1/4}} e^{-x^2/8}, \quad x \in \mathbb{R}.
$$

II. *A nonlinear case ($\beta > 0$) with a harmonic oscillator potential,*

$$
V(x) = \frac{x^2}{2}, \quad \beta = 60, \quad \phi_0(x) = \frac{1}{(\pi)^{1/4}} e^{-x^2/2}, \quad x \in \mathbb{R}.
$$

Case I is solved on $\Omega = [-16, 16]$ and Case II on $\Omega = [-8, 8]$ with mesh size $h = 1/32$. Figure 4.1 shows the evolution of the energy $E_\beta(\phi)$ for different time steps k and different numerical methods.

From Figure 4.1, the following observations can be made:

(1) BEFD is an implicit method, and energy diminishing is observed for both the linear and the nonlinear cases under any time step $k > 0$. The error in the ground state solution is only due to the second-order spatial discretization.
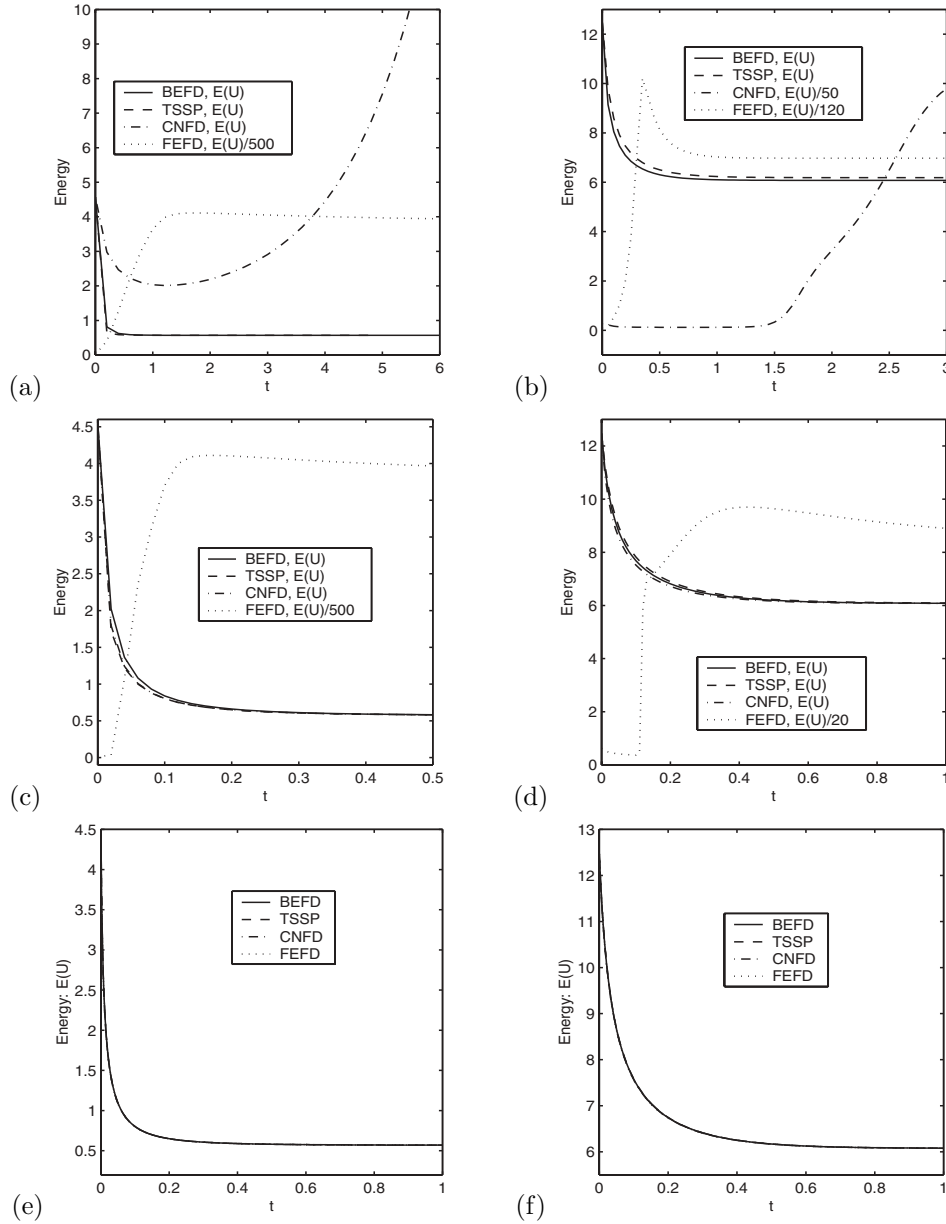
FIG. 4.1. *Energy evolution in Example* 4.1. *Left column for case* I: (a) $k = 0.2$, (c) $k = 0.02$, *and* (e) $k = 0.0005$. *Right column for case* II: (b) $k = 0.05$, (d) $k = 0.01$, *and* (f) $k = 0.0005$.

(2) TSSP is an explicit method, and energy diminishing is observed for the linear case under any time step $k > 0$. For the nonlinear case, our numerical experiments show that $k < \frac{1}{\beta}$ guarantees energy diminishing. The error in the ground state solution is caused by both the spatial discretization, which is spectrally accurate, and time splitting, which is second-order accurate. From an accuracy point of view, large values of k should be prohibited.

(3) CNFD is an implicit method and FEFD is an explicit method. For both

schemes, energy diminishing is observed only when the time step k satisfies the conditions (3.17) and (3.18), respectively.

To summarize briefly, in general, BEFD is much better than CNFD for computing the ground state solution because BEFD is monotone for any $k > 0$ and CNFD is *not*. TSSP is much better than FEFD. In practice, one can use either BEFD or TSSP. BEFD allows the use of a much bigger time step k which does *not* depend on $\beta \geq 0$, but the scheme has only second-order accuracy in space. At each time step, a linear system is solved. In the appendix, we give the detailed BEFD discretization in two and three dimensions when the potential $V(\mathbf{x})$ and the initial data $\phi_0(\mathbf{x})$ have symmetry with/without a central vortex state in the condensate. TSSP is explicit, easy to program, less demanding on memory, and spectrally accurate in space, but it needs a small time step k which depends on the accuracy required and the value of $\beta > 0$ but not on the mesh size h. Based on our numerical experiments given in the next subsection, both methods work very well for computing the ground state solution of BEC.
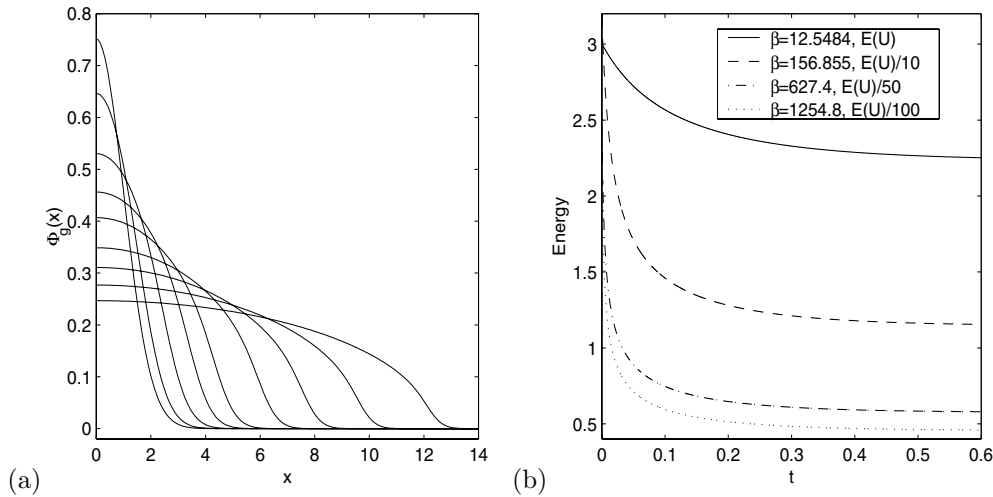

Fig. 4.2. *Ground state solution ϕ_g in Example 4.2.* (a) *For $\beta = 0$, 3.1371, 12.5484, 31.371, 62.742, 156.855, 313.71, 627.42, 1254.8 (with decreasing peak).* (b) *Energy evolution for different β.*

4.2. Applications to ground state solutions.

Example 4.2. Ground state solution of one-dimensional BECs with harmonic oscillator potential

$$V(x) = \frac{x^2}{2}, \quad \phi_0(x) = \frac{1}{(\pi)^{1/4}} e^{-x^2/2}, \quad x \in \mathbb{R}.$$

The CNGF (2.15)–(2.16) with $d = 1$ is solved on $\Omega = [-16, 16]$ with mesh size $h = 1/8$ and time step $k = 0.001$ by using TSSP. The steady state solution is reached when $\max |\Phi^{n+1} - \Phi^n| < \varepsilon = 10^{-6}$. Figure 4.2 shows the ground state solution $\phi_g(x)$ and energy evolution for different β. Table 4.1 displays the values of $\phi_g(0)$, radius mean square x_{rms}, energy $E_\beta(\phi_g)$, and chemical potential μ_g.

The results in Figure 4.2 and Table 4.1 agree very well with the ground state solutions of BEC obtained by directly minimizing the energy functional [6]. BEFD gives the same results with $k = 0.1$.

TABLE 4.1

Maximum value of the wave function $\phi_g(0)$, root mean square size x_{rms}, energy $E_\beta(\phi_g)$, and ground state chemical potential μ_g versus the interaction coefficient β in one dimension.

β	$\phi_g(0)$	x_{rms}	$E_\beta(\phi_g)$	$\mu_g = \mu_\beta(\phi_g)$
0	0.7511	0.7071	0.5000	0.5000
3.1371	0.6463	0.8949	1.0441	1.5272
12.5484	0.5301	1.2435	2.2330	3.5986
31.371	0.4562	1.6378	3.9810	6.5587
62.742	0.4067	2.0423	6.2570	10.384
156.855	0.3487	2.7630	11.464	19.083
313.71	0.3107	3.4764	18.171	30.279
627.42	0.2768	4.3757	28.825	48.063
1254.8	0.2467	5.5073	45.743	76.312

Example 4.3. Ground state solution of BECs in two dimensions. Two cases are considered:

I. *With a harmonic oscillator potential* [6, 7, 19], *i.e.,*

$$V(x,y) = \frac{1}{2}(\gamma_x^2 x^2 + \gamma_y^2 y^2).$$

II. *With a harmonic oscillator potential and a potential of a stirrer corresponding to a far-blue detuned Gaussian laser beam* [24] *which is used to generate vortices in BEC* [9], *i.e.,*

$$V(x,y) = \frac{1}{2}(\gamma_x^2 x^2 + \gamma_y^2 y^2) + w_0 e^{-\delta((x-r_0)^2 + y^2)}.$$

The initial condition is chosen as

$$\phi_0(x,y) = \frac{(\gamma_x \gamma_y)^{1/4}}{\pi^{1/2}} e^{-(\gamma_x x^2 + \gamma_y y^2)/2}.$$

For case I, we choose $\gamma_x = 1$, $\gamma_y = 4$, $w_0 = \delta = r_0 = 0$, $\beta = 200$ and solve the problem by TSSP on $\Omega = [-8, 8] \times [-4, 4]$ with mesh size $h_x = 1/8$, $h_y = 1/16$ and time step $k = 0.001$. We get the following results from the ground state solution ϕ_g:

$$x_{\mathrm{rms}} = 2.2734, \ y_{\mathrm{rms}} = 0.6074, \ \phi_g^2(\mathbf{0}) = 0.0808, \ E_\beta(\phi_g) = 11.1563, \ \mu_g = 16.3377.$$

For case II, we choose $\gamma_x = 1$, $\gamma_y = 1$, $w_0 = 4$, $\delta = r_0 = 1$, $\beta = 200$ and solve the problem by TSSP on $\Omega = [-8, 8]^2$ with mesh size $h = 1/8$ and time step $k = 0.001$. We get the following results from the ground state solution ϕ_g:

$$x_{\mathrm{rms}} = 1.6951, \quad y_{\mathrm{rms}} = 1.7144, \quad \phi_g^2(\mathbf{0}) = 0.034, \quad E_\beta(\phi_g) = 5.8507, \quad \mu_g = 8.3269.$$

In addition, Figure 4.3 shows surface plots of the ground state solution ϕ_g. BEFD gives similar results with $k = 0.1$.

Example 4.4. Ground state solution of BECs in three dimensions. Two cases are considered:

I. *With a harmonic oscillator potential* [6, 7, 19], *i.e.,*

$$V(x,y,z) = \frac{1}{2}(\gamma_x^2 x^2 + \gamma_y^2 y^2 + \gamma_z^2 z^2).$$
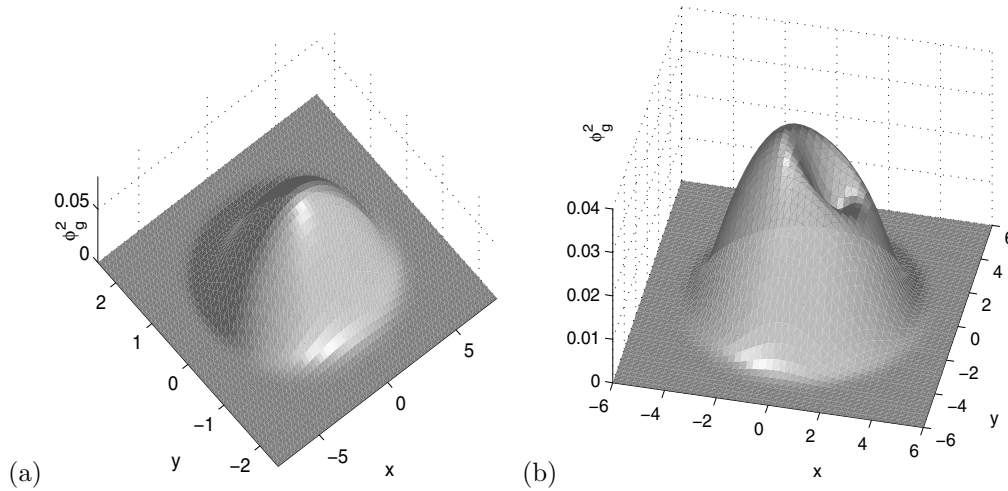
Fig. 4.3. *Ground state solutions* ϕ_g^2 *in Example* 4.3 *for* (a) *case* I *and* (b) *case* II.

II. *With a harmonic oscillator potential and a potential of a stirrer corresponding to a far-blue detuned Gaussian laser beam* [24, 10] *which is used to generate vortex in BECs* [10], *i.e.,*

$$V(x,y,z) = \frac{1}{2}(\gamma_x^2 x^2 + \gamma_y^2 y^2 + \gamma_z^2 z^2) + w_0 e^{-\delta((x-r_0)^2 + y^2)}.$$

The initial condition is chosen as

$$\phi_0(x,y,z) = \frac{(\gamma_x \gamma_y \gamma_z)^{1/4}}{\pi^{3/4}} e^{-(\gamma_x x^2 + \gamma_y y^2 + \gamma_z z^2)/2}.$$

For case I, we choose $\gamma_x = 1$, $\gamma_y = 2$, $\gamma_z = 4$, $w_0 = \delta = r_0 = 0$, $\beta = 200$ and solve the problem by TSSP on $\Omega = [-8, 8] \times [-6, 6] \times [-4, 4]$ with mesh size $h_x = \frac{1}{8}$, $h_y = \frac{3}{32}$, $h_z = \frac{1}{16}$ and time step $k = 0.001$. The ground state solution ϕ_g gives

$$x_{\text{rms}} = 1.67, \ y_{\text{rms}} = 0.87, \ z_{\text{rms}} = 0.49, \ \phi_g^2(\mathbf{0}) = 0.052, \ E_\beta(\phi_g) = 8.33, \ \mu_g = 11.03.$$

For case II, we choose $\gamma_x = 1$, $\gamma_y = 1$, $\gamma_z = 2$, $w_0 = 4$, $\delta = r_0 = 1$, $\beta = 200$ and solve the problem by TSSP on $\Omega = [-8, 8]^3$ with mesh size $h = \frac{1}{8}$ and time step $k = 0.001$. The ground state solution ϕ_g gives

$$x_{\text{rms}} = 1.37, \ y_{\text{rms}} = 1.43, \ z_{\text{rms}} = 0.70, \ \phi_g^2(\mathbf{0}) = 0.025, \ E_\beta(\phi_g) = 5.27, \ \mu_g = 6.71.$$

Furthermore, Figure 4.4 shows surface plots of the ground state solution $\phi_g^2(x, 0, z)$. BEFD gives similar results with $k = 0.1$.

Example 4.5. Two-dimensional central vortex states in BECs, i.e.,

$$V(x,y) = V(r) = \frac{1}{2}\left(\frac{m^2}{r^2} + r^2\right), \quad \phi_0(x,y) = \phi_0(r) = \frac{1}{\sqrt{\pi m!}} r^m e^{-r^2/2}, \quad 0 \le r.$$

The CNGF (2.15)–(2.16) is solved in polar coordinate with $\Omega = [0, 8]$ with mesh size $h = \frac{1}{64}$ and time step $k = 0.1$ by using BEFD (for details see Appendix A.3). Figure 4.5a shows the ground state solution $\phi_g(r)$ with $\beta = 200$ for different index of the central vortex m. Table 4.2 displays the values of $\phi_g(0)$, radius mean square r_{rms}, energy $E_\beta(\phi_g)$, and chemical potential μ_g.
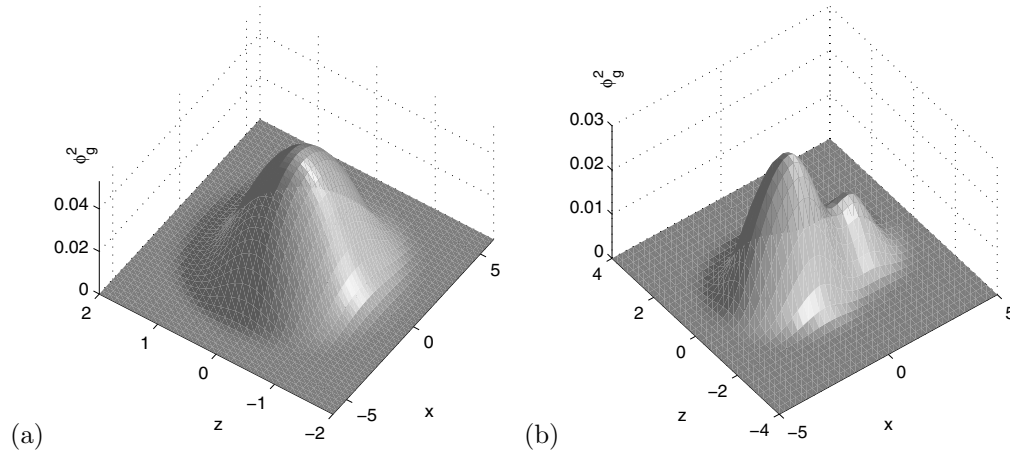
FIG. 4.4. *Ground state solutions $\phi_g^2(x, 0, z)$ in Example 4.4 for* (a) *case* I *and* (b) *case* II.
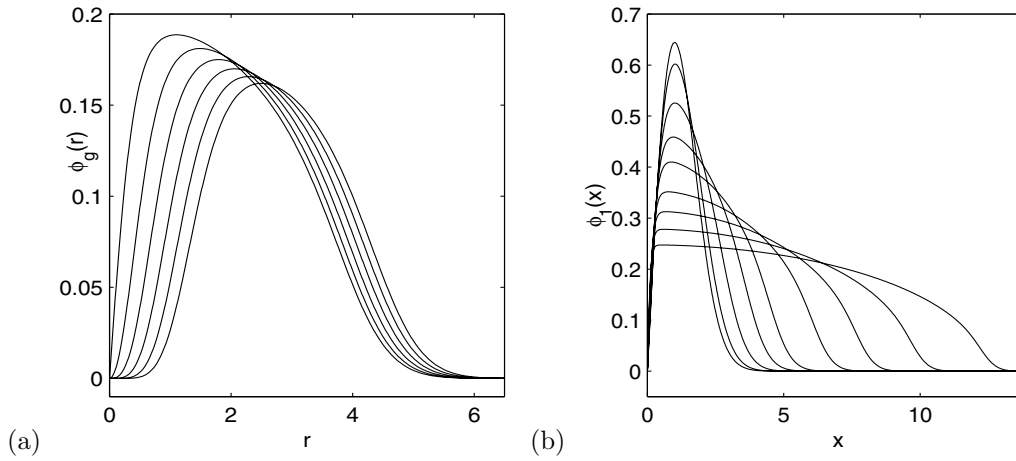

FIG. 4.5. (a) *Two-dimensional central vortex states $\phi_g(r)$ in Example 4.5. $\beta = 200$ for $m = 1$ to 6 (with decreasing peak).* (b) *First excited state solution $\phi_1(x)$ (an odd function) in Example 4.6. For $\beta = 0$, 3.1371, 12.5484, 31.371, 62.742, 156.855, 313.71, 627.42, 1254.8 (with decreasing peak).*

TABLE 4.2
Numerical results for two-dimensional central vortex states in BECs.

Index m	$\phi_g(0)$	r_{rms}	$E_\beta(\phi_g)$	$\mu_g = \mu_\beta(\phi_g)$
1	0.0000	2.4086	5.8014	8.2967
2	0.0000	2.5258	6.3797	8.7413
3	0.0000	2.6605	7.0782	9.3160
4	0.0000	2.8015	7.8485	9.9772
5	0.0000	2.9438	8.6660	10.6994
6	0.0000	3.0848	9.5164	11.4664

4.3. Application to compute the first excited state. Let the eigenfunctions of the nonlinear eigenvalue problem (1.6), (1.7) under the constraint (1.8) be

$$\pm\phi_g(\mathbf{x}), \pm\phi_1(\mathbf{x}), \pm\phi_2(\mathbf{x}), \ldots,$$

with their energies satisfy

$$E_\beta(\phi_g) < E_\beta(\phi_1) < E_\beta(\phi_2) < \cdots .$$

Then ϕ_j is called as the jth excited state solution. In fact, ϕ_g and ϕ_j $(j = 1, 2, \ldots)$ are critical points of the energy functional $E_\beta(\phi)$ under the constraint (1.8). In one dimension, when $V(x) = \frac{x^2}{2}$ is chosen as the harmonic oscillator potential, the first excited state solution $\phi_1(x)$ is a real odd function, and $\phi_1(x) = \frac{\sqrt{2}}{(\pi)^{1/4}} x\, e^{-x^2/2}$ when $\beta = 0$ [27]. We observe numerically that the CNGF (2.15)–(2.16) and its BEFD discretization (3.4) can also be applied directly to compute the first excited state solution, i.e., $\phi_1(x)$, provided that the initial data $\phi_0(x)$ in (2.16) is chosen as an odd function. Here we only present a preliminary numerical example in one dimension. Extensions to two and three dimensions are straightforward.

Example 4.6. The first excited state solution of BECs in one dimension with a harmonic oscillator potential, i.e.,

$$V(x) = \frac{x^2}{2}, \quad \phi_0(x) = \frac{\sqrt{2}}{(\pi)^{1/4}} x\, e^{-x^2/2}, \quad x \in \mathbb{R}.$$

The CNGF (2.15)–(2.16) with $d = 1$ is solved on $\Omega = [-16, 16]$ with mesh size $h = 1/64$ and time step $k = 0.1$ by using BEFD. Figure 4.5b shows the first excited state solution $\phi_1(x)$ for different β. Table 4.3 displays the radius mean square $x_{\mathrm{rms}} = \|x\phi_1\|_{L^2(\Omega)}$, ground state and first excited state energies $E_\beta(\phi_g)$ and $E_\beta(\phi_1)$, ratio $E_\beta(\phi_1)/E_\beta(\phi_g)$, chemical potentials $\mu_g = \mu_\beta(\phi_g)$ and $\mu_1 = \mu_\beta(\phi_1)$, and ratio μ_1/μ_g.

TABLE 4.3
Numerical results for the first excited state solution in one dimension in Example 4.6.

β	x_{rms}	$E_\beta(\phi_g)$	$E_\beta(\phi_1)$	$\frac{E_\beta(\phi_1)}{E_\beta(\phi_g)}$	μ_g	μ_1	$\frac{\mu_1}{\mu_g}$
0	1.2247	0.500	1.500	3.000	0.500	1.500	3.000
3.1371	1.3165	1.044	1.941	1.859	1.527	2.357	1.544
12.5484	1.5441	2.233	3.037	1.360	3.598	4.344	1.207
31.371	1.8642	3.981	4.743	1.192	6.558	7.279	1.110
62.742	2.2259	6.257	6.999	1.119	10.38	11.089	1.068
156.855	2.8973	11.46	12.191	1.063	19.08	19.784	1.037
313.71	3.5847	18.17	18.889	1.040	30.28	30.969	1.023
627.42	4.4657	28.82	29.539	1.025	48.06	48.733	1.014
1254.8	5.5870	45.74	46.453	1.016	76.31	76.933	1.008

From the results in Table 4.3 and Figure 4.5b, we can see that the BEFD can be applied directly to compute the first excited states in BECs. Furthermore, we have

$$\lim_{\beta\to+\infty} \frac{E_\beta(\phi_1)}{E_\beta(\phi_g)} = 1, \qquad \lim_{\beta\to+\infty} \frac{\mu_1}{\mu_g} = 1.$$

These results are confirmed with the results in [6], where the ground and first excited states are computed by directly minimizing the energy functional through the finite element discretization.

5. Conclusions. We presented a CNGF and examined its energy diminishing property, numerical discretization, and relation to the imaginary time method. Our study here provided some mathematical justification of the imaginary time integration method used in the physics literature to compute the ground state solution of BECs. The BEFD and TSSP methods were proposed to discretize the CNGF. Comparison between the two proposed methods and existing methods showed that BEFD and TSSP are much better for the computation of the BEC ground state solution. Numerical results in one, two, and three dimensions with different types of potentials used in BEC were reported to demonstrate the effectiveness of the BEFD and TSSP methods. We also observed that the CNGF and its BEFD discretization can be used directly to compute the first excited state in BECs provided that the initial data is chosen as an odd function. Furthermore, extension of the CNGF and its BEFD discretization to compute higher excited states with an orthonormalization technique is on-going.

Appendix. BEFD discretization in BECs when $V(\mathbf{x})$ has symmetry. In this appendix, we present detailed BEFD discretizations for the CNGF in BECs in two and three dimensions when the potential $V(\mathbf{x})$ and the initial data $\phi_0(\mathbf{x})$ have symmetry with/without a central vortex state in the condensate. Choose $R > 0$, $a < b$, and time step $k > 0$ with $|a|$, b, R sufficiently large. Denote the mesh size $h_r = (R - 0)/M$ and $h_z = (b - a)/N$ with M and N two positive integers, time steps $t_n = n\,k$, $n = 0, 1, \ldots$, and grid points $r_j = jh_r$, $j = 0, 1, \ldots, M$, and $r_{j-\frac{1}{2}} = (j - \frac{1}{2})h_r$, $j = 0, 1, \ldots, M + 1$, $z_l = a + l\,h_z$, $l = 0, 1, \ldots, N$.

A.1. Two dimensions with radial symmetry and three dimensions with spherical symmetry. $V(\mathbf{x}) = V(r)$ and $\phi_0(\mathbf{x}) = \phi_0(r)$ with $r = |\mathbf{x}|$ and $\Omega = \mathbb{R}^d$ with $d = 2, 3$ in (2.15)–(2.16). In this case, the solution $\phi(\mathbf{x}, t) = \phi(r, t)$ and the GFDN collapses to a one-dimensional problem:

$$(A.1) \quad \phi_t = \frac{1}{2r^{d-1}}\frac{\partial}{\partial r}\left(r^{d-1}\frac{\partial \phi}{\partial r}\right) - V(r)\phi - \beta|\phi|^2\phi, \quad 0 < r < \infty, \; t_n < t < t_{n+1},$$

$$(A.2) \quad \phi_r(0, t) = 0, \quad \lim_{r \to \infty} \phi(r, t) = 0, \quad t \geq 0,$$

$$(A.3) \quad \phi(r, t_{n+1}) \triangleq \frac{\phi(r, t_{n+1}^-)}{\|\phi(\cdot, t_{n+1}^-)\|}, \quad 0 < r < \infty, \; n \geq 0,$$

$$(A.4) \quad \phi(r, 0) = \phi_0(r) \geq 0, \quad 0 < r < \infty,$$

where $\|\phi_0\| = 1$ and the norm $\|\cdot\|$ is defined as

$$\|\phi\|^2 = C_d \int_0^\infty \phi^2(r, t)r^{d-1}dr, \quad \text{with } C_d = \begin{cases} 2\pi, & d = 2, \\ 4\pi, & d = 3. \end{cases}$$

The BEFD discretization of (A.1)–(A.4) is

$$\frac{\phi^*_{j-\frac{1}{2}} - \phi^n_{j-\frac{1}{2}}}{k} = \frac{1}{2\,h_r^2\,r^{d-1}_{j-\frac{1}{2}}}\left[r^{d-1}_j\phi^*_{j+\frac{1}{2}} - \left(r^{d-1}_j + r^{d-1}_{j-1}\right)\phi^*_{j-\frac{1}{2}} + r^{d-1}_{j-1}\phi^*_{j-\frac{3}{2}}\right]$$

$$- V\left(r_{j-\frac{1}{2}}\right)\phi^*_{j-\frac{1}{2}} - \beta\left(\phi^n_{j-\frac{1}{2}}\right)^2\phi^*_{j-\frac{1}{2}}, \quad j = 1, \ldots, M - 1,$$

$$(A.5) \quad \phi^*_{-\frac{1}{2}} = \phi^*_{\frac{1}{2}}, \qquad \phi^*_{M-\frac{1}{2}} = 0,$$

$$\phi^{n+1}_{j-\frac{1}{2}} = \frac{\phi^*_{j-\frac{1}{2}}}{\|\phi^*\|}, \quad j = 0, \ldots, M, \; n = 0, 1, \ldots,$$

$$\phi^0_{j-\frac{1}{2}} = \phi_0(r_j), \quad j = 1, \ldots, M, \quad \phi^0_{-\frac{1}{2}} = \phi^0_{\frac{1}{2}},$$

where the norm is defined as

$$\|\phi^*\|^2 = h_r C_d \sum_{j=1}^{M} \left(\phi_{j-\frac{1}{2}}^*\right)^2 r_{j-\frac{1}{2}}^{d-1}.$$

A.2. Three dimensions with cylindrical symmetry. $V(\mathbf{x}) = V(r,z)$ and $\phi_0(\mathbf{x}) = \phi_0(r,z)$ with $r = \sqrt{x^2 + y^2}$ and $\Omega = \mathbb{R}^d$ with $d = 3$ in (2.15)–(2.16). This is the most popular case in the setup of current BEC experiments. In this case, the solution $\phi(\mathbf{x},t) = \phi(r,z,t)$ (and the GFDN) collapses to a two-dimensional problem with $0 < r < \infty$ and $-\infty < z < \infty$:

(A.6) $\quad \phi_t = \frac{1}{2}\left[\frac{1}{r}\frac{\partial}{\partial r}\left(r\frac{\partial \phi}{\partial r}\right) + \frac{\partial^2 \phi}{\partial z^2}\right] - V(r,z)\phi - \beta|\phi|^2\phi, \quad t_n < t < t_{n+1},$

(A.7) $\quad \phi_r(0,z,t) = 0, \quad \lim_{r\to\infty} \phi(r,z,t) = 0, \quad \lim_{z\to\pm\infty} \phi(r,z,t) = 0, \quad t \geq 0,$

(A.8) $\quad \phi(r,z,t_{n+1}) \triangleq \dfrac{\phi(r,z,t_{n+1}^-)}{\|\phi(\cdot,t_{n+1}^-)\|}, \quad n \geq 0,$

(A.9) $\quad \phi(r,z,0) = \phi_0(r,z) \geq 0,$

where $\|\phi_0\| = 1$ and the norm $\|\cdot\|$ is defined as

$$\|\phi\|^2 = 2\pi \int_0^\infty \int_{-\infty}^\infty \phi^2(r,z,t) r\, dz\, dr.$$

The BEFD discretization of (A.6)–(A.9) is

$$\frac{\phi_{j-\frac{1}{2}\,l}^* - \phi_{j-\frac{1}{2}\,l}^n}{k} = \frac{1}{2\,h_r^2\,r_{j-\frac{1}{2}}}\left[r_j\,\phi_{j+\frac{1}{2}\,l}^* - (r_j + r_{j-1})\phi_{j-\frac{1}{2}\,l}^* + r_{j-1}\,\phi_{j-\frac{3}{2}\,l}^*\right]$$

$$+ \frac{1}{2h_z^2}\left[\phi_{j-\frac{1}{2}\,l+1}^* - 2\phi_{j-\frac{1}{2}\,l}^* + \phi_{j-\frac{1}{2}\,l-1}^*\right] - V(r_{j-\frac{1}{2}}, z_l)\,\phi_{j-\frac{1}{2}\,l}^*$$

$$- \beta\left(\phi_{j-\frac{1}{2}\,l}^n\right)^2 \phi_{j-\frac{1}{2}\,l}^*, \quad j = 1,\ldots,M-1,\ l = 1,2\ldots,N-1,$$

(A.10)
$$\phi_{-\frac{1}{2}\,l}^* = \phi_{\frac{1}{2}\,l}^*, \quad \phi_{M-\frac{1}{2}\,l}^* = 0, \quad l = 1,2,\ldots,N-1,$$

$$\phi_{j-\frac{1}{2}\,0}^* = \phi_{j-\frac{1}{2}\,M}^* = 0, \quad j = 0,1,\ldots,M,$$

$$\phi_{j-\frac{1}{2}\,l}^{n+1} = \frac{\phi_{j-\frac{1}{2}\,l}^*}{\|\phi^*\|}, \quad j = 0,\ldots,M,\ l = 0,1,\ldots,N,\ n = 0,1,\ldots,$$

(A.11) $\quad \phi_{j-\frac{1}{2}\,l}^0 = \phi_0(r_{j-\frac{1}{2}}, z_l), \ \phi_{-\frac{1}{2}\,l}^0 = \phi_{\frac{1}{2}\,l}^0, \ j = 1,\ldots,M,\ l = 0,\ldots,N,$

where the norm is defined as

$$\|\phi^*\|^2 = 2\pi h_r h_z \sum_{j=1}^{M} \sum_{l=1}^{N-1} \left(\phi_{j-\frac{1}{2}\,l}^*\right)^2 r_{j-\frac{1}{2}}.$$

To find a stationary vortex solution of (1.1), one plugs the ansatz

$$\psi(\mathbf{x},t) = \begin{cases} e^{-i\mu t}\,e^{im\theta}\,\phi(r), & d = 2, \\ e^{-i\mu t}\,e^{im\theta}\,\phi(r,z), & d = 3, \end{cases} \quad r = \sqrt{x^2 + y^2},$$

into (1.1) instead of (1.5), where $m > 0$ an integer corresponding to the index of the vortex. For more details related to central vortex states in BECs, we refer to [16, 30, 32].

A.3. Two-dimensional central vortex states in BECs. $V(\mathbf{x}) = V(r) = \frac{1}{2}(\frac{m^2}{r^2} + r^2)$ and $\phi_0(\mathbf{x}) = \phi_0(r)$ with $\phi_0(0) = 0$, $r = \sqrt{x^2 + y^2}$, and $\Omega = \mathbb{R}^2$ in (2.15)–(2.16). In this case, the solution $\phi(\mathbf{x}, t) = \phi(r, t)$ and the GFDN collapses to a one-dimensional problem:

(A.12) $\quad \phi_t = \dfrac{1}{2r} \dfrac{\partial}{\partial r} \left(r \dfrac{\partial \phi}{\partial r} \right) - V(r)\phi - \beta|\phi|^2\phi, \quad 0 < r < \infty, \ t_n < t < t_{n+1},$

(A.13) $\quad \phi(0, t) = 0, \quad \lim_{r \to \infty} \phi(r, t) = 0, \quad t \geq 0,$

(A.14) $\quad \phi(r, t_{n+1}) \triangleq \dfrac{\phi(r, t_{n+1}^-)}{\|\phi(\cdot, t_{n+1}^-)\|}, \quad 0 < r < \infty, \ n \geq 0,$

(A.15) $\quad \phi(r, 0) = \phi_0(r) \geq 0, \quad 0 < r < \infty, \quad \left(\text{e.g.}, = \dfrac{1}{\sqrt{\pi m!}} r^m e^{-r^2/2} \right),$

where $\phi(0) = 0$, $\|\phi_0\| = 1$, and the norm $\| \cdot \|$ is defined as

$$\|\phi\|^2 = 2\pi \int_0^\infty \phi^2(r, t) r \, dr.$$

The BEFD discretization of (A.12)–(A.15) is

(A.16)
$$\frac{\phi_j^* - \phi_j^n}{k} = \frac{1}{2\, h_r^2\, r_j} \left[r_{j+\frac{1}{2}}\, \phi_{j+1}^* - \left(r_{j+\frac{1}{2}} + r_{j-\frac{1}{2}}\right)\phi_j^* + r_{j-\frac{1}{2}}\, \phi_{j-1}^* \right]$$
$$- V(r_j)\, \phi_j^* - \beta\left(\phi_j^n\right)^2 \phi_j^*, \quad j = 1, \ldots, M-1,$$
$$\phi_j^{n+1} = \frac{\phi_j^*}{\|\phi^*\|}, \quad j = 0, \ldots, M, \ n = 0, 1, \ldots,$$
$$\phi_0^* = \phi_M^* = 0,, \quad \phi_j^0 = \phi_0(r_j), \quad j = 0, 1, \ldots, M,$$

where the norm is defined as

$$\|\phi^*\|^2 = 2\pi h_r \sum_{j=1}^{M-1} r_j(\phi_j^*)^2.$$

A.4. Three-dimensional central vortex states in BECs. $V(\mathbf{x}) = V(r, z) = \frac{1}{2}(\frac{m^2}{r^2} + \gamma_r^2 r^2 + \gamma_z^2 z^2)$ and $\phi_0(\mathbf{x}) = \phi_0(r, z)$ with $\phi_0(0, z) = 0$ for $z \in \mathbb{R}$, $\gamma_r > 0$, $\gamma_z > 0$ constants, $r = \sqrt{x^2 + y^2}$, and $\Omega = \mathbb{R}^3$ in (2.15)–(2.16). In this case, the solution $\phi(\mathbf{x}, t) = \phi(r, z, t)$ and the GFDN collapses to a two-dimensional problem with $0 < r < \infty$ and $-\infty < z < \infty$:

(A.17) $\quad \phi_t = \dfrac{1}{2} \left[\dfrac{1}{r} \dfrac{\partial}{\partial r} \left(r \dfrac{\partial \phi}{\partial r} \right) + \dfrac{\partial^2 \phi}{\partial z^2} \right] - V(r, z)\phi - \beta\phi^3, \quad t_n < t < t_{n+1},$

(A.18) $\quad \phi(0, z, t) = 0, \quad \lim_{r \to \infty} \phi(r, z, t) = 0, \quad \lim_{z \to \pm\infty} \phi(r, z, t) = 0, \quad t \geq 0,$

(A.19) $\quad \phi(r, z, t_{n+1}) \triangleq \dfrac{\phi(r, z, t_{n+1}^-)}{\|\phi(\cdot, t_{n+1}^-)\|}, \quad n \geq 0,$

(A.20) $\quad \phi(r, z, 0) = \phi_0(r, z) \geq 0, \quad \left(\text{e.g.}, = \dfrac{\gamma_z^{1/4} \gamma_r^{(m+1)/2}}{\pi^{3/4}(m!)^{1/2}} r^m\, e^{-(\gamma_r r^2 + \gamma_z z^2)/2} \right),$

where $\phi_0(0, z) = 0$ for $z \in \mathbb{R}$, $\|\phi_0\| = 1$, and the norm $\|\cdot\|$ is defined as

$$\|\phi\|^2 = 2\pi \int_0^\infty \int_{-\infty}^\infty \phi^2(r, z, t) r \, dz \, dr.$$

The BEFD discretization of (A.17)–(A.20) is

$$\frac{\phi_{j\,l}^* - \phi_{j\,l}^n}{k} = \frac{1}{2\,h_r^2\,r_j}\Big[r_{j+\frac{1}{2}}\,\phi_{j+1\,l}^* - \big(r_{j+\frac{1}{2}} + r_{j-\frac{1}{2}}\big)\phi_{j\,l}^* + r_{j-\frac{1}{2}}\,\phi_{j-1\,l}^*\Big]$$

$$+ \frac{1}{2h_z^2}\Big[\phi_{j\,l+1}^* - 2\phi_{j\,l}^* + \phi_{j\,l-1}^*\Big] - V(r_j, z_l)\phi_{j\,l}^* - \beta(\phi_{j\,l}^n)^2\phi_{j\,l}^*,$$

$$j = 1, \ldots, M-1, \ l = 1, 2\ldots, N-1,$$

(A.21)
$$\phi_{0\,l}^* = \phi_{M\,l}^* = 0, \quad l = 0, 1, \ldots, N, \qquad \phi_{j\,0}^* = \phi_{j\,M}^* = 0, \quad j = 1, 1, \ldots, M-1,$$

$$\phi_{j\,l}^{n+1} = \frac{\phi_{j\,l}^*}{\|\phi^*\|}, \quad j = 0, \ldots, M, \ l = 0, 1, \ldots, N, \ n = 0, 1, \ldots,$$

$$\phi_{j\,l}^0 = \phi_0(r_j, z_l), \quad j = 0, \ldots, M, \ l = 0, \ldots, N,$$

where the norm is defined as

$$\|\phi^*\|^2 = 2\pi h_r h_z \sum_{j=1}^{M-1} \sum_{l=1}^{N-1} (\phi_{j\,l}^*)^2\,r_j.$$

The linear system at every time step in sections A.1 and A.3 can be solved by the Thomas algorithm, and those in sections A.2 and A.4 can be solved by the Gauss–Seidel iterative method.

REFERENCES

[1] S.K. ADHIKARI, *Numerical solution of the two-dimensional Gross–Pitaevskii equation for trapped interacting atoms*, Phys. Lett. A, 265 (2000), pp. 91–96.

[2] A. AFTALION AND Q. DU, *Vortices in a rotating Bose–Einstein condensate: Critical angular velocities and energy diagrams in the Thomas–Fermi regime*, Phys. Rev. A, 64 (2001), article 063603.

[3] J.R. ANGLIN AND W. KETTERLE, *Bose–Einstein condensation of atomic gases*, Nature, 416 (2002), pp. 211–218.

[4] W. BAO, S. JIN, AND P.A. MARKOWICH, *On time-splitting spectral approximations for the Schrödinger equation in the semiclassical regime*, J. Comput. Phys., 175 (2002), pp. 487–524.

[5] W. BAO, S. JIN, AND P.A. MARKOWICH, *Numerical study of time-splitting spectral discretizations of nonlinear Schrödinger equations in the semiclassical regimes*, SIAM J. Sci. Comput., 25 (2003), pp. 27–64.

[6] W. BAO AND W. TANG, *Ground state solution of trapped interacting Bose–Einstein condensate by directly minimizing the energy functional*, J. Comput. Phys., 187 (2003), pp. 230–254.

[7] W. BAO, D. JAKSCH, AND P.A. MARKOWICH, *Numerical solution of the Gross–Pitaevskii equation for Bose–Einstein condensation*, J. Comput. Phys., 187 (2003), pp. 318–342.

[8] W. BAO AND D. JAKSCH, *An explicit unconditionally stable numerical methods for solving damped nonlinear Schrödinger equations with a focusing nonlinearity*, SIAM J. Numer. Anal., 41 (2003), pp. 1406–1426.

[9] B.M. CARADOC-DAVIS, R.J. BALLAGH, AND K. BURNETT, *Coherent dynamics of vortex formation in trapped Bose–Einstein condensates*, Phys. Rev. Lett., 83 (1999), pp. 895–898.

[10] B.M. CARADOC-DAVIS, R.J. BALLAGH, AND P.B. BLAKIE, *Three-dimensional vortex dynamics in Bose–Einstein condensates*, Phys. Rev. A, 62 (2000), article 011602.

[11] M.M. CERIMELE, M.L. CHIOFALO, F. PISTELLA, S. SUCCI, AND M.P. TOSI, *Numerical solution of the Gross–Pitaevskii equation using an explicit finite-difference scheme: An application to trapped Bose–Einstein condensates*, Phys. Rev. E, 62 (2000), pp. 1382–1389.

[12] M.M. Cerimele, F. Pistella, and S. Succi, *Particle-inspired scheme for the Gross–Pitaevskii equation: An application to Bose–Einstein condensation*, Comput. Phys. Comm., 129 (2000), pp. 82–90.

[13] M.L. Chiofalo, S. Succi, and M.P. Tosi, *Ground state of trapped interacting Bose–Einstein condensates by an explicit imaginary-time algorithm*, Phys. Rev. E, 62 (2000), pp. 7438–7444.

[14] E. Cornell, *Very cold indeed: The nanokelvin physics of Bose–Einstein condensation*, J. Res. Natl. Inst. Stan., 101 (1996), pp. 419–434.

[15] F. Dalfovo, S. Giorgini, L.P. Pitaevskii, and S. Stringari, *Theory of Bose–Einstein condensation in trapped gases*, Rev. Modern Phys., 71 (1999), pp. 463–512.

[16] F. Dalfovo and S. Stringari, *Bosons in anisotropic traps: Ground state and vortices*, Phys. Rev. A, 53 (1996), pp. 2477–2485.

[17] R.J. Dodd, *Approximate solutions of the nonlinear Schrödinger equation for ground and excited states of Bose–Einstein condensates*, J. Res. Natl. Inst. Stan., 101 (1996), pp. 545–552.

[18] Q. Du, *Numerical computations of quantized vortices in Bose–Einstein condensate*, in Recent Progress in Computational and Applied PDEs, T. Chan et al., eds., Kluwer Academic, Dordrecht, The Netherlands, 2002, pp. 155–168.

[19] M. Edwards and K. Burnett, *Numerical solution of the nonlinear Schrödinger equation for small samples of trapped neutral atoms*, Phys. Rev. A, 51 (1995), pp. 1382–1386.

[20] A. Gammal, T. Frederico, and L. Tomio, *Improved numerical approach for the time-independent Gross–Pitaevskii nonlinear Schrödinger equation*, Phys. Rev. E, 60 (1999), pp. 2421–2424.

[21] G.H. Golub and C.F. Van Loan, *Matrix Computations*, Johns Hopkins University Press, Baltimore, MD, 1989.

[22] M. Greiner, O. Mandel, T. Esslinger, T.W. Hänsch, and I. Bloch, *Quantum phase transition from a superfluid to a Mott insulator in a gas of ultracold atoms*, Nature, 415 (2002), pp. 39–45.

[23] E.P. Gross, *Structure of a quantized vortex in boson systems*, Nuovo Cimento, 20 (1961), pp. 454–477.

[24] B. Jackson, J.F. McCann, and C.S. Adams, *Vortex formation in dilute inhomogeneous Bose–Einstein condensates*, Phys. Rev. Lett., 80 (1998), pp. 3903–3906.

[25] D. Jaksch, C. Bruder, J.I. Cirac, C.W. Gardiner, and P. Zoller, *Cold bosonic atoms in optical lattices*, Phys. Rev. Lett., 81 (1998), pp. 3108–3111.

[26] L. Landau and E. Lifschitz, *Quantum Mechanics: Non-Relativistic Theory*, Pergamon Press, New York, 1977.

[27] I.N. Levine, *Quantum Chemistry*, 5th ed., Prentice-Hall, New York, 1991.

[28] E.H. Lieb, R. Seiringer, and J. Yngvason, *Bosons in a trap: A rigorous derivation of the Gross–Pitaevskii energy functional*, Phys. Rev. A, 61 (2000), article 043602.

[29] F.-H. Lin and Q. Du, *Ginzburg–Landau vortices: Dynamics, pinning, and hysteresis*, SIAM J. Math. Anal., 28 (1997), pp. 1265–1293.

[30] E. Lundh, C.J. Pethick, and H. Smith, *Vortices in Bose–Einstein-condensed atomic clouds*, Phys. Rev. A, 59 (1998), pp. 4816–4823.

[31] L.P. Pitaevskii, *Vortex lines in an imperfect Bose gas*, Soviet Phys. JETP, 13 (1961), pp. 451–454.

[32] D.S. Rokhsar, *Vortex stability and persistent currents in trapped Bose gas*, Phys. Rev. Lett., 79 (1997), pp. 2164–2167.

[33] P.A. Ruprecht, M.J. Holland, K. Burrett, and M. Edwards, *Time-dependent solution of the nonlinear Schrödinger equation for Bose-condensed trapped neutral atoms*, Phys. Rev. A, 51 (1995), pp. 4704–4711.

[34] B.I. Schneider and D.L. Feder, *Numerical approach to the ground and excited states of a Bose–Einstein condensed gas confined in a completely anisotropic trap*, Phys. Rev. A, 59 (1999), pp. 2232–2242.

[35] L. Simon, *Asymptotics for a class of nonlinear evolution equations, with applications to geometric problems*, Ann. Math. (2), 118 (1983), pp. 525–571.

[36] C. Sulem and P.L. Sulem, *The Nonlinear Schrödinger Equation: Self-focusing and Wave Collapse*, Springer-Verlag, New York, 1999.